VIII International Conference on Fracture Mechanics of Concrete and Concrete Structures
FraMCoS-8
J.G.M. Van Mier, G. Ruiz, C. Andrade, R.C. Yu and X.X. Zhang (Eds)

AN APPROPRIATE INDICATOR FOR BOND STRENGTH DEGRADATION DUE TO REINFORCEMENT CORROSION

CHRISTIAN FISCHER[*], JOŠKO OŽBOLT[†]

[*] Materials Testing Institute (MPA), University of Stuttgart
Pfaffenwaldring 2, 70569 Stuttgart, Germany
e-mail: christian.fischer@mpa.uni-stuttgart.de, www.mpa.uni-stuttgart.de

[†] Institute of Construction Materials (IWB), University of Stuttgart
Pfaffenwaldring 4, 70569 Stuttgart, Germany
e-mail: ozbolt@iwb.uni-stuttgart.de, www.iwb.uni-stuttgart.de

Key words: bond strength, reinforcement corrosion, crack width, corrosion penetration

Abstract: In the paper an appropriate indicator for degradation of bond strength due to corrosion of reinforcement is investigated. Common indicators, which are currently in use, are the mass loss and the average corrosion penetration of steel. The crack width in concrete cover is not frequently used as an indicator of corrosion induced damage in bond. A comparison between the average corrosion penetration and the crack width in concrete cover with respect to bond strength is discussed. For this reason, experimental and numerical investigations on beam-end specimens were carried out. Within the experimental investigations the specimens were corroded to different states before bars were pulled-out. A modest corrosion rate close to the maximum natural corrosion rate under splash conditions was chosen. Maximum values of current density were between 15 and 25 µA/cm². In addition investigations on morphology and distribution of corrosion products in the vicinity of the reinforcement surface were performed. In numerical investigations a detailed 3D-FE model was employed. The reinforcement is discretized by 3D finite elements. In order to model expansion, due to different levels of corrosion, 1D radial contact elements on the reinforcement-concrete contact surface were used. The contact elements can take up axial compressive forces and shear forces due to friction between reinforcement and concrete. In the numerical analyses the damage due to the radial expansion of corrosion products is simulated first. This is modeled by radial expansion of the contact elements. Subsequently, the reinforcement bar is pulled-out from the concrete beam-end specimen. The study confirms that the crack width is a good indicator for the degradation of bond resistance due to corrosion of reinforcement. The bond strength is dependent on the concrete confinement and thus on the crack state of the surrounding concrete. In fact from the mechanical point of view crack width should be a better indicator for degradation of bond strength, however, the difficulty is the fact that crack width depends on bar diameter and concrete cover.

1 INTRODUCTION

Bond degradation due to corrosion of reinforcement embedded in concrete is an ongoing topic. There is a large number of reinforced concrete structures, which are already degraded due to corrosion of steel reinforcement or at which there is a major risk of deterioration due to corrosion of steel reinforcement. Although a tremendous amount of investigations was conducted notably within the past two decades there are still a number of open questions.

The principal effects of reinforcement corrosion on bond performance have been ascer-

tained. These include the following facts: the pressure due to volumetric expansion of corrosion products may initially result in increasing bond strength at average corrosion penetration of x_{corr} < 25 – 50 µm (loss of bar radius), depending on the cover/bar ratio (*c/d*-ratio). With increasing corrosion the tensile hoop stresses in the surrounding concrete exceed the tensile strength, longitudinal cracks start to split the concrete cover and the bond strength is decreasing [1, 2, 3, 4]. The rate of decrease can be reduced or even reversed into a certain increase of bond strength due to a transverse reinforcement [4, 5, 6, 7, 8]. The transverse reinforcement ensures an additional confinement which is limited by loss of cross section of the transverse reinforcement. The increase of bond strength with increasing corrosion, which was found in some cases, is due to the pretension of stirrup arms [9] and increasing friction coefficient between rebar and concrete [10].

Experimental results on the change in bond strength with increasing corrosion have a wide scatter. Beside the two major reasons (i) use of different specimens and (ii) a wide range of corrosion accelerations used, the parameter indicating the change in bond strength with increasing corrosion might be a reason as well. This assumption was investigated and is discussed in the present paper.

2 SPECIMEN GEOMETRY AND TYPES

According to the recommendations of Chana [11] a beam-end specimen was chosen. The experimental investigations were performed on specimens with four bars diameter 12 mm and 16 mm placed in corner positions with concrete covers of 20 mm and 35 mm, respectively, see Figure 1. The two combinations of bar diameter and concrete cover were designed without stirrups in fact, two different types have been investigated, see Table 1. The specimens had a bond length of 180 mm. For each type eight specimens were cast. The bars of two specimens were tested without corrosion (reference tests) and the bars of six specimens were tested at different corrosion states within a period of 16 months. The four bars of each specimen were pulled-out load controlled one after each other beginning with the top cast bars. Mutually diagonally arranged bars were pulled-out in the same direction.

The concrete used had a cement content of 360 kg/m³, a water/cement ratio of 0.5 and a maximum aggregate grain size of 8 mm. The resulting material parameters of concrete and the parameters of the reinforcement steel are shown in Table 2. To proceed depassivation of the reinforcement, a chloride content of 2.5 % per weight of cement was added to the concrete.

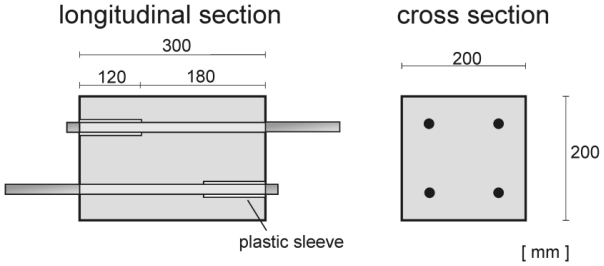

Figure 1: Geometry of beam end specimen

Table 1: Specimen types

Type No.	*d* mm	*c* mm	*c/d* -
12/20	12	20	1,67
16/35	16	35	2,19

Table 2: Concrete and steel parameters

concrete				steel	
f_{cm} MPa	f_{ct} MPa	E MPa	G_F J/m²	f_y MPa	R_m MPa
41	3.3	29,400	180	500	600

a) b)

Figure 2: Crack pattern after bar pull-out of a) a type 12/20 reference specimen and b) a type 12/20 specimen after 16 months of corrosion

In order to accelerate the corrosion process, a potential of +500 mV NHE was applied between the rebars (anodes) and two platinized titanium meshes (cathodes) one at each side of the specimen. Twice a day the two longitudinal sides of each specimen were wetted with 1 % chloride solution for 1 and 3 minutes. The resulting current densities for bar diameter d = 12 mm were around i_{corr} = 20-25 μA/cm^2, and for bar diameter d = 16 mm they were about i_{corr} = 15-20 μA/cm^2. Due to this sensitive conditioning, maximum crack widths of around w = 1.3 mm at corrosion penetration depths of around x_{corr} = 400-500 μm were reached after a corrosion time of 16 months.

In Figure 2 the crack pattern after bar pull-out of a type 12/20 reference specimen with d = 12 mm and c = 20 mm and a type 12/20 specimen after 16 month of corrosion time are shown. In both cases failure was reached due to splitting of the concrete cover.

3 NUMERICAL MODEL

The numerical calculations were performed with the FE-code MASA [12]. For concrete the microplane material model was used. The results presented in the paper are based on the following detailed 3D model. The model taken for numerical calculation was geometrically identical to the beam end specimen used for the experimental investigations except, for the sake of simplicity, only one bar was modeled, see Figure 3a.

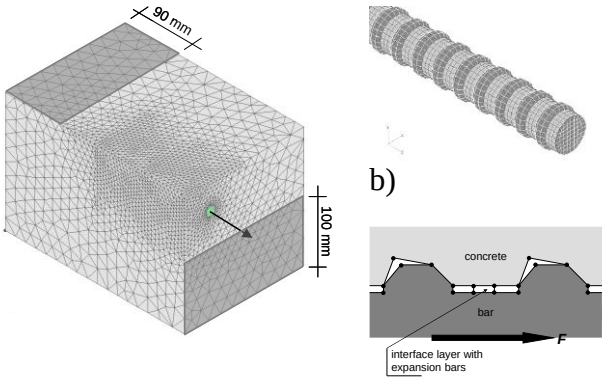

Figure 3: Detailed FE-model with a) discretization and constraints of full model, b) detail of bar discretization and c) schematic view of bar-interface-concrete area.

The reinforcement bar was modeled by 3D solid elements with a simplified axially symmetric rib geometry, see Figure 3b. To clarify the transition between rebar and surrounding concrete a detail is illustrated in Figure 3c. Hence it becomes apparent that the load transfer between steel and concrete is performed by the rib front faces. No transfer of tension forces can occur at the rib back faces. The expansion of the corrosion products and the lateral pressure dependent Mohr-Coulomb friction component was modeled by an interface layer within the rib dales, see Figure 3c.

The expansion of the corrosion products simulated by the above mentioned interface layer was assumed to be uniformly distributed around the bar circumference as well as over the bond length and defined by the following equation:

$$\Delta r = -r + \sqrt{r^2 + (k_{v,eff} - 1) \cdot (2r \cdot x_{corr} - x_{corr}^2)} \qquad (1)$$

With Δr as the free radius increase dependent on bar radius r, effective volume ratio (volume factor) between corrosion product and iron $k_{v,eff}$ and average corrosion penetration depth x_{corr}. Experimental investigations (mentioned under chapter 4.2) and numerical calibration of the model resulted in $k_{v,eff}$ = 1.5. Another important value is the stiffness of the corrosion products. In the literature there are values mentioned between 100 to 500 MPa [13] and 215,000 to 350,000 MPa [14] depending on the structure of the investigated sample. The low values come from the granular structure of corrosion products. The high values are measured at crystalline level. However, the stiffness applied for the numerical investigations was chosen to E_{corr} = 250 MPa since this value gave best agreement between numerical and experimental results within the calibration.

The simulation was performed in two stages. First the expansion of the interface layer was performed to the respective corrosion expansion level. The elemental expansion was kept to this stage during bar pull out. Afterwards the bar was pulled out at increments of 0.08 mm, whereas the load was transferred by the rib front faces. Due to the cracked concrete

cover and the lack of lateral pressure almost no load transfer took place at interface layer within the rib dales.

The calibration of the model was obtained by simulating the experimental types 1 and 3. As a result concrete parameters shown in Table 2 (except G_F) were increased by around 10 %. The reason for this correction is found in the very small element size at the interface, which is rather small to present macroscopic concrete characteristics, which is intended by the microplane model.

Numerical simulations were carried out for variety of bar diameter-concrete cover combinations, see Table 3. For two of the nine combinations experimental results were obtained.

Table 3: Geometrical variations of numerical simulations and experiments

d mm	*c* mm	*c/d* -	experimental type
12	12	1.0	-
	20	1.7	12/20
	36	3.0	-
14	14	1.0	-
	28	2.0	-
	42	3.0	-
16	16	1.0	-
	35	2.2	16/35
	48	3.0	-

4 EXPERIMENTAL RESULTS

4.1 Effects on bond strength

The large differences between the results of corrosion affecting bond strength of different research teams are the major problem and makes assessment of uniform standards difficult to obtain. For this reason, own experimental results are compared to the results from the literature. As evaluation parameters for the effects on bond strength the average corrosion penetration and the crack width are considered. By comparing different results it was ensured that always the same or similar bar diameter and concrete cover were compared.

The average corrosion penetration was calculated from the gravimetrically obtained mass loss by the following equation:

$$x_{corr} = \sqrt{\frac{m_0}{\pi \cdot L \cdot \rho}} - \sqrt{\frac{m_0 - \Delta m}{\pi \cdot L \cdot \rho}} \qquad (2)$$

The average corrosion penetration in Equation (2) is calculated from the original mass m_0, the mass loss due to corrosion Δm, the bond length L and the density of the steel ρ. The crack width was measured at the end of the conditioning time directly before bar pull-out. Measurement was performed at three points over the crack length by means of a crack magnifier. In case of two cracks, one on each side of the concrete faces, the sum of both was taken into account, see Figure 4.

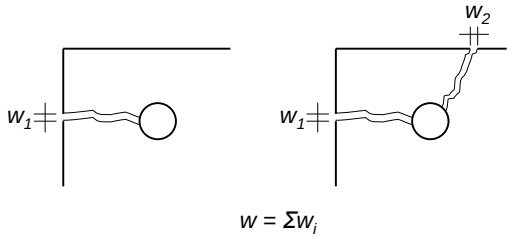

Figure 4: Measurement of crack width

In Figure 5 the normalized bond strength is plotted over the average corrosion penetration and over the crack width. Results of Rodriguez et al. [8] and own investigations with bar diameters of 16 mm are shown. Bond strength plotted over the average corrosion penetration gives no correlation between the two sets of results, see Figure 5a. However, plotting the same results over the crack width, see Figure 5b, an almost perfect correlation was found. Similar results were found by comparing other diameters [9]. Hence the crack width as indicating parameter for the change in bond strength due to reinforcement corrosion shows advantages compared to the average corrosion penetration.

This raises the question about the reason for the better correlation with crack width as indicating parameter. In this context it should be noted that the crack width has the great advantage of being a non-destructive determinable parameter. However, to find an answer for the previous question investigations on nature and distribution of corrosion products have been performed. They are presented in the following chapter.

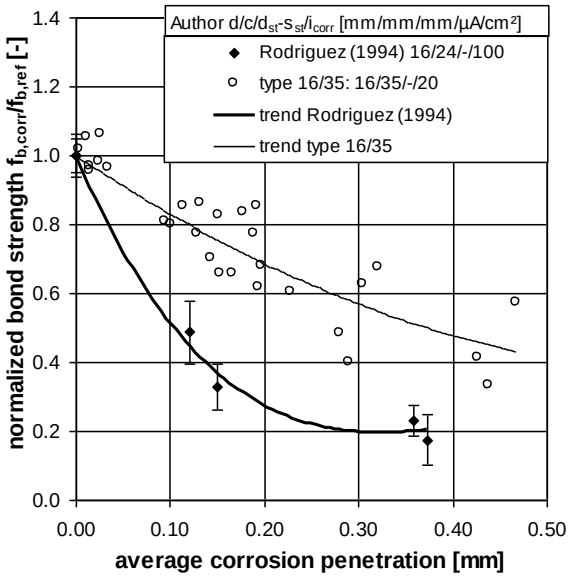

a)

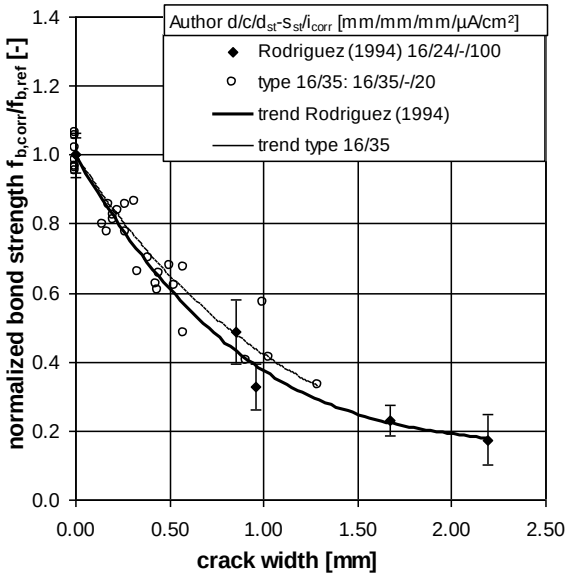

b)

Figure 5: Bond strength values of Rodriguez et al. [8] compared to own results for 16 mm bars a) over average corrosion penetration and b) over crack width

4.2 Nature and distribution of the corrosion products

Almost all investigations on the influence of corrosion on bond strength are based on accelerated corrosion conditioning. Acceleration factors vary between the 10- and 2,000-fold of the maximum natural corrosion rate [9]. Hence nature and distribution of corrosion products of so conditioned specimens might differ from corrosion products developed under natural corrosion. In contrast to previous investigations the corrosion rate of the present investigation was between 15 and 25 µA/cm² and thus at most 5-fold the maximum natural value of 5 µA/cm² [15].

Within the present investigations the emerged corrosion products have been analyzed with aid of Raman spectroscopy and compared to corrosion products developed under natural conditions. For this, a thin section of the transition zone of steel-rust-concrete was analyzed, see Figure 6. In this picture a dense rust layer between steel and concrete developed which is the source for the expansion pressure and thus the cracks in the concrete cover. With the aid of Raman spectroscopy the major corrosion products of this layer were identified as goethite (α-FeOOH) with inclusions of lepidocrocite (γ-FeOOH). Same findings were made by Chitty et al. [16] at archeological artefacts of reinforcement in concrete corroded under natural conditions.

However, corrosion products are not only kept at the steel surface but penetrate into pores and cracks of the surrounding concrete, see Figure 7. Thus there is only a certain amount of corrosion products to build up the expansion pressure causing the cracks in concrete. However, the cracks directly indicate the loss of bond strength whereas the corrosion penetration indicates the total amount of corrosion.

This finding is quantified by comparing the nominal volume factor k_v (volumetric factor between corrosion product and iron) and the effective volume factor $k_{v,eff}$ (the volume factor responsible for the corrosion expansion). The nominal volume factor for goethite and lepidocrocite is around $k_v = 3$. The effective volume factor obtained from the experimental investigations is around $k_{v,eff} = 1.35$ [9]. It follows that only around 45 % of the total corrosion products are responsible for the corrosion expansion pressure, which initiates concrete cracking and loss of bond strength. This value was obtained at testing conditions comparable to a maritime splash zone. Changing these conditions may alter this value.

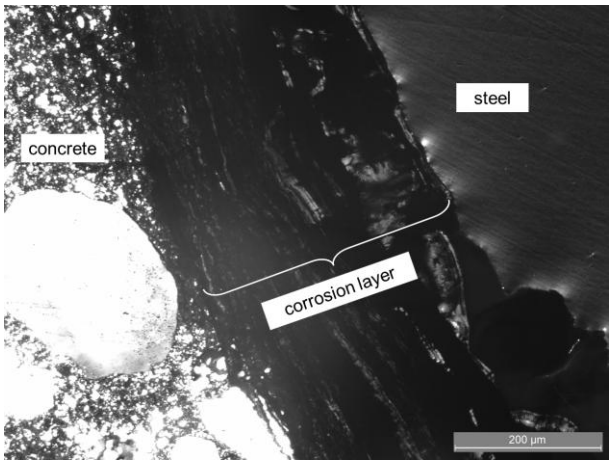

Figure 6: Microscopic picture of a thin section of transition zone concrete-rust-steel (removed)

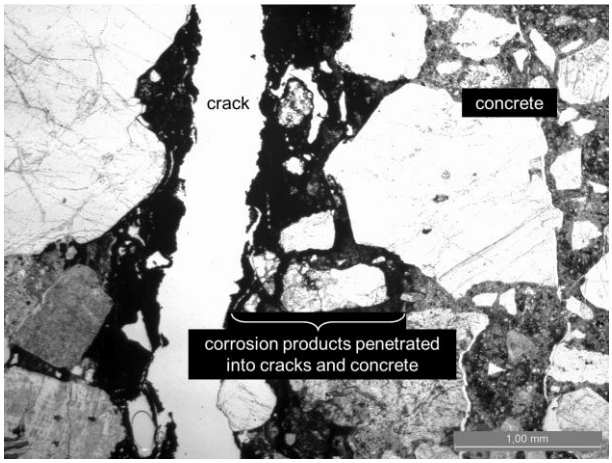

Figure 7: Microscopic picture of a thin section of a crack zone in the concrete indicating widely distributed corrosion products

5 NUMERICAL RESULTS

In addition to the experimental investigations numerical simulations were performed. Within the simulations a variety of three different bar diameters each with three different concrete covers were analyzed, see Table 3.

In Figure 10, 9 and 10 results of bond strengths over average crack width for bar diameters 12 mm, 14 mm and 16 mm each with *c/d*-ratios of around 1, 2 and 3 are shown. From these figures it becomes apparent that the simulations of the experimental types 12/20 and 16/35 are showing a good correlation. However, simulations of bar diameter 12 mm are rather conservative at high corrosion levels compared to experimental results. Furthermore, it is found that the change of bond strength over crack width depends on both (i) bar diameter and (ii) concrete cover. The larger the bar diameter is the more consistent is the loss of bond strength, especially at higher corrosion levels. The decrease of bond strength at small corrosion levels intensifies with increasing concrete cover. The reason is explained in more detail in [9, 17]. It follows that the crack width is a good indicator for the loss of bond strength, however, the intensity of the loss depends on both the bar diameter and the concrete cover.

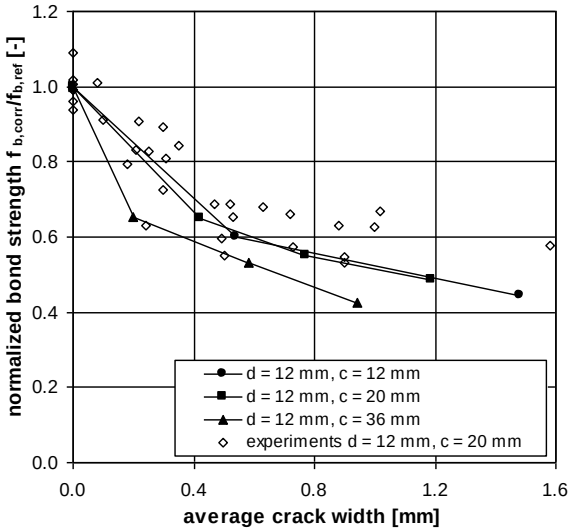

Figure 8: Normalized bond strength over average crack width of simulations and experiments with 12 mm bar diameter and *c/d*-ratios of around 1, 2 and 3

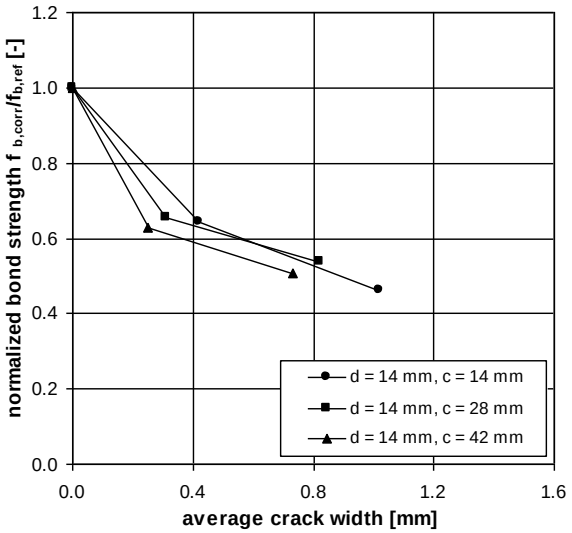

Figure 9: Normalized bond strength over average crack width of simulations with 14 mm bar diameter and *c/d*-ratios of around 1, 2 and 3

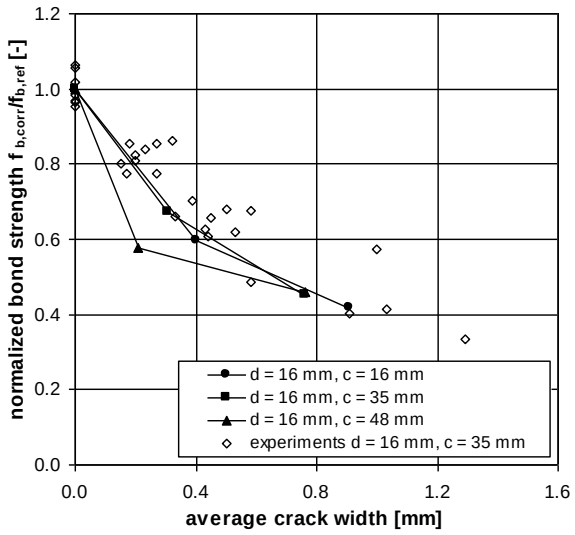

Figure 10: Normalized bond strength over average crack width of simulations and experiments with 16 mm bar diameter and *c/d*-ratios of around 1, 2 and 3

6 CONCLUSION

The reinforcement corrosion of concrete structures involves many different aspects and one is the effect on bond behavior. Within this topic the assessment of bond degradation plays an important role. To assess the objective indicator for the bond reduction caused by corrosion in the paper the average corrosion penetration and the crack width are compared. It turns out that the crack width better represents the reduction of bond strength. This was particularly clear in the comparison of results from different researchers. Based on the numerical results the decrease of bond strength showed a dependency of both the bar diameter and the concrete cover. An increasing bar diameter results in an overall higher loss of bond strength. However, increasing concrete cover tends to a stronger decline of bond strength already at small levels of corrosion.

ACKNOWLEDGMENT

The presented results are obtained within the DFG research project 537 “Modeling reinforcement corrosion”. The authors wish to thank the German Research Foundation (DFG).

REFERENCES

[1] Almusallam, A. A.; Al-Ghatani, A. S.; Aziz, A.-R.; Rasheeduzzafar 1996. Effect of reinforcement corrosion on bond strength. *Construction and Building Materials*, 10 (2), pp. 123–129.

[2] Auyeung, Y., Balaguru, P. & Chung, L. 2000. Bond Behavior of Corroded Reinforcement Bars. *ACI Materials Journal*, 97 (2), pp. 214–220.

[3] Fang, C.;Lundgren, K.; Chen, L.; Zhu, C. 2004. Corrosion influence on bond in reinforced concrete. *Cement and Concrete Research*, 34 (11), pp. 2159–2167.

[4] Cabrera J. G. & Ghoddoussi, P. 1992. The effect of reinforcement corrosion on the strength of the steel/concrete "bond". In: *Bond in Concrete. Proceedings of the International Conference*, pp. 10/11-10/24.

[5] Al-Sulaimani, G. J.; Kaleemullah, M.; Basunbul, I. A.; Rsheeduzzafar 1990. Influence of Corrosion and Cracking on Bond Behavior and Strength of Reinforced Concrete Members. *ACI Structural Journal*, 87 (2), pp. 220–231.

[6] Berra, M., Castellani, A. & Coronelli, D. 1997. Bond in reinforced concrete and corrosion of bars. In: *Structural Falts and Repair. Proceedings of the 7th International Conference. Edinburgh, UK: Engineering Technics Press*, pp. 349–356.

[7] Mangat, P. S.; Elgraf, M. S. 1999. Bond characteristics of corroding reinforcement in concrete beams. In: *Materials and Structures*, 32, pp. 89–97.

[8] Rodriguez, J., Ortega, L. M. & Casal, J. 1994. Corrosion of reinforcing bars and service life of reinforced concrete structures: corrosion and bond deterioration. In: *Proceedings of the International Conference on Concrete Across Borders, Odense, Denmark*, pp. 315–326.

[9] Fischer, C. 2012. Influences of reinforcement corrosion on bond between steel and concrete (In German). Stuttgart University, http://elib.uni-stuttgart.de/opus/frontdoor.php?source_opus=7547, Dissertation, 2012.

[10] Cairns, J., Du, Y. & Law, D. 2007. Influence of corrosion on the friction characteristics of the steel/concrete interface. *International Journal of Construction and Building Materials*, 21 (1), pp. 190–197.

[11] Chana, P. S. 1990. A test method to establish realistic bond stresses. *Magazine of Concrete Research*, 42 (151), pp. 83–90.

[12] Ožbolt, J. 1998. MASA-Macroscopic Space Analysis.Report to describe the FE-code MASA. Stuttgart, University.

[13] Suda, K.; Misra, S.; Motohashi, K. 1993. Corrosion products of reinforcing bars embedded in concrete. Advances in Corrosion and Protection. In: *Corrosion Science* 35 (5-8), pp. 1543–1549.

[14] Samsonov, G. V. 1973. The oxide handbook. New York, London: IFI/Plenum.

[15] Balabanic, G.; Bicanic, N.; Durekovic, A. 1996. Mathematical modeling of electrochemical steel corrosion in concrete. In: *Journal of Engineering Mechanics* 122 (12), pp. 1113-1122.

[16] Chitty, W.-J.; Dillmann, P.; L'Hostis, V.; Lombard, C. 2005. Long-term corrosion resistance of metallic reinforcements in concrete – a study of corrosion mechanisms based on archaeological artefacts. In: Corrosion Science 47 (6), pp. 1555-1581.

[17] Fischer, C.; Ožbolt, J. 2012. Influence of bar diameter and concrete cover on bond degradation due to corrosion. In: *Bond in Concrete 2012. Proceedings of the International Conference*, pp. 445-451.